

# SEARCH FOR FRAGMENTED M1 STRENGTH IN THE $^{48}\text{Ca}(p,p')$ REACTION

D.J. Mercer

*University of Colorado, Boulder, Colorado 80303*

G.M. Crawley, S. Danczyk, A. Galonsky, and J. Wang

*National Superconducting Cyclotron Laboratory, East Lansing, Michigan 48824*

A. Bacher, G.P.A. Berg, A.C. Betker, W. Schmidt, and E.J. Stephenson

*Indiana University Cyclotron Facility, Bloomington, Indiana 47408*

The quenching of M1 ( $\Delta L = 0, \Delta J^\pi = 1^+$ ) strength remains one of the outstanding problems in nuclear physics. If configuration mixing within and across major shells is a dominant mechanism for quenching, then one should be able to locate fragmented M1 strength close to where the main strength occurs. In  $^{48}\text{Ca}(p,p')$  there is a single strong peak at 10.21 MeV that contains 30% of the predicted total strength, but no fragmented strength has been found.<sup>1,2</sup> In contrast, the strength in  $^{44}\text{Ca}$ ,  $^{42}\text{Ca}$ , and  $^{40}\text{Ca}$  has been found to be completely fragmented into states near 10 MeV. Data from  $^{48}\text{Ca}(e,e')$  experiments<sup>3,4</sup> suggest the possibility of up to eighteen weak transitions, each with strength less than 4% as large as the 10.21 MeV transition. Recent shell model studies<sup>5</sup> also predict such fragmented strength. The present experiment is designed to verify or disprove the existence of this fragmented M1 strength using  $^{48}\text{Ca}(p,p')$ .

Previous  $^{48}\text{Ca}(p,p')$  experiments have not been sensitive enough to small M1 transitions to reproduce the  $(e,e')$  results. In some,<sup>2,6,7</sup> the resolution was quite good, but the bombarding energy was well below 100 MeV where the reaction mechanism is not particularly selective of spin-flip transitions; in others<sup>1,8</sup> the bombarding energy is above 160 MeV but the experimental background is too high. In Fig. 1 is a spectrum from Ref. 1 showing the difficulty with background at a very forward scattering angle. The  $\nu(f_{5/2}, f_{7/2}^{-1})$  10.21-MeV peak is clearly visible, but any small peaks containing less than 5% of the strength of the 10.21 MeV peak would disappear into the background.

A signature of an M1 transition is a  $(p,p')$  cross section that increases as the scattering angle approaches  $0^\circ$ . Higher  $\Delta L$  multipoles have cross sections which decrease (or at least do not increase so fast) as the angle approaches  $0^\circ$ . With careful selection of bombarding energy, we can discriminate against non spin-flip ( $\Delta L = 0, \Delta J^\pi = 0^+$ ) transitions, at least six of which are known to occur in the energy region of interest.<sup>2</sup> Thus, by studying the very forward angular distributions from inelastic scattering of 200 MeV protons, we hope to identify any M1 transitions. In 1993 we collected  $^{48}\text{Ca}(p,p')$  data at  $9.1^\circ$ ,  $7.1^\circ$ ,  $5.1^\circ$  and  $4.1^\circ$  using the K-600 Spectrometer at the Indiana University Cyclotron Facility (IUCF).<sup>9</sup> In 1994 we attempted the more difficult task of collecting high-statistics, low-background data near  $0^\circ$  using the K-600 Spectrometer in transmission mode.

A schematic of the K-600 spectrometer set for transmission mode appears in Fig. 2. Both the scattered particles and the unscattered beam are transmitted through the spectrometer. The spectrometer fields are set so that the protons from inelastic scattering are dispersed according to momentum at the focal plane. Four wire chambers (X1, Y1, X2,

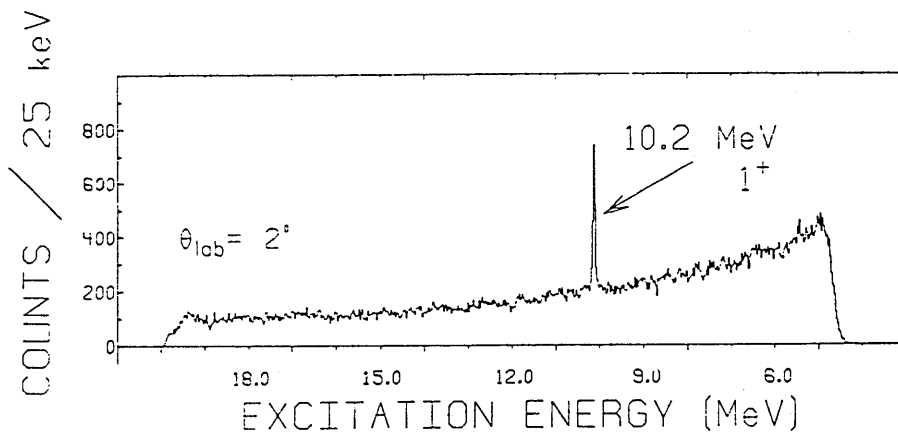


Figure 1. Spectrum from Ref. 1 showing the strong  $1^+$  peak in  $^{48}\text{Ca}(p,p')$  at a very forward angle. Experimental background hides possible smaller peaks containing less than 5% of the strength in the main peak.

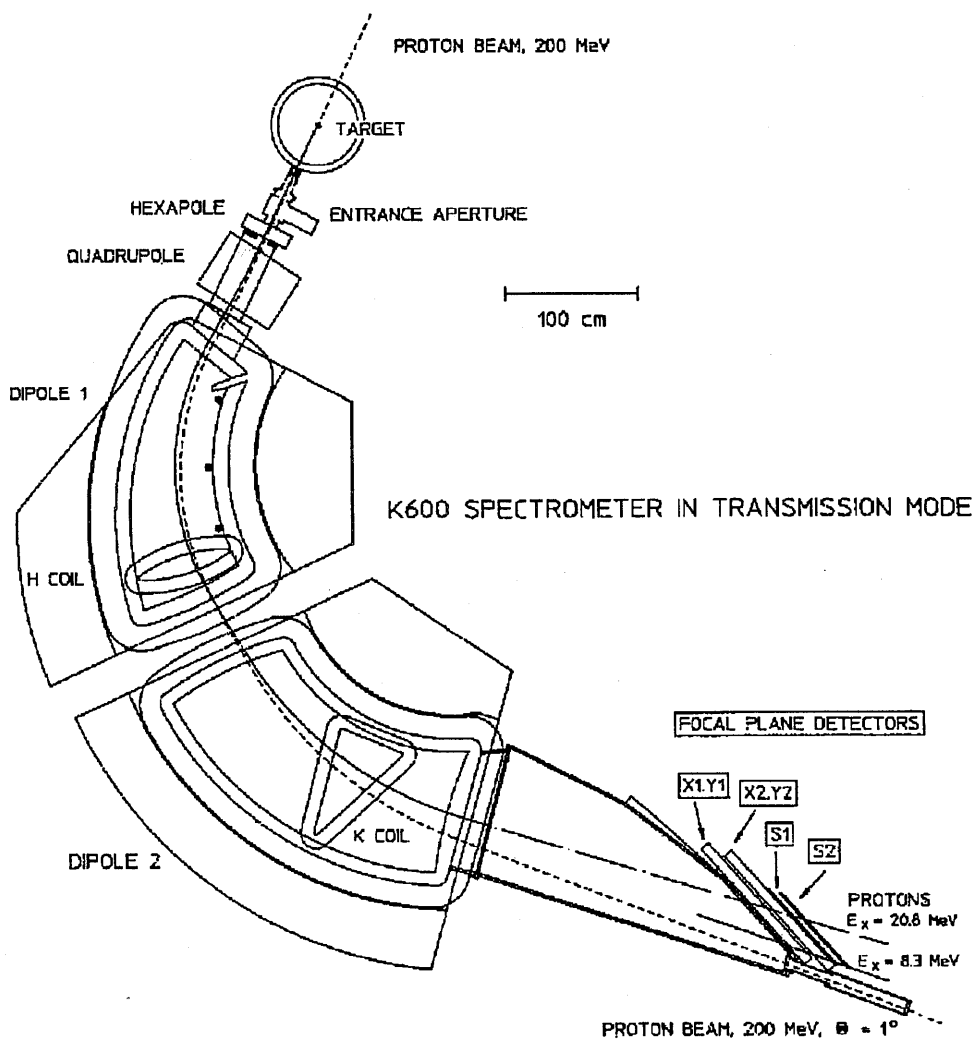


Figure 2. Diagram of the IUCF K-600 spectrometer in transmission mode.

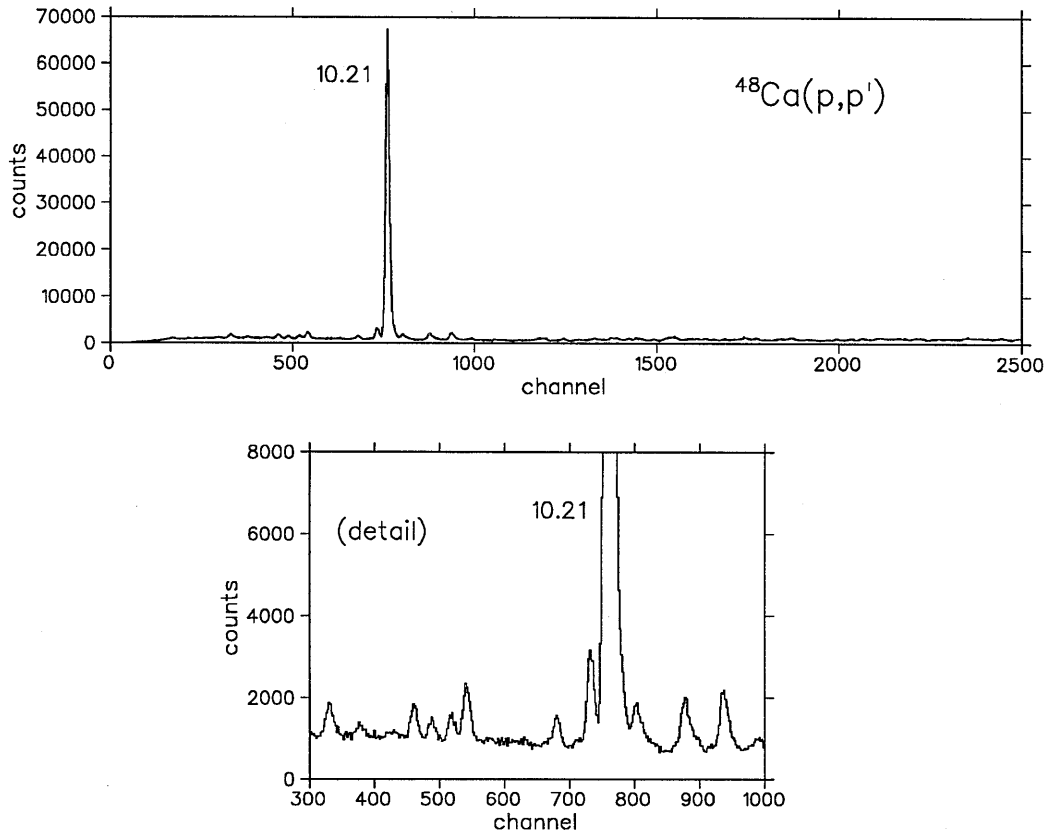


Figure 3. On-line spectrum from the  $^{48}\text{Ca}(p,p')$  reaction at very forward angles and a bombardment energy of 200 MeV. Channels 0-2500 span roughly 8.0–15.7 MeV of excitation energy. Besides the strong 10.21 MeV peak, at least ten smaller peaks are visible, some of which may contain fragmented M1 strength. The lower panel is an expanded view of the upper panel near 10.21 MeV.

and Y2) and two scintillator paddles (S1, S2) provide tracking and particle identification. To reconstruct the very small scattering angles (ranging from  $0^\circ$  to  $2^\circ$ ), both horizontal (X) and vertical (Y) components of the tracks must be determined. The unscattered beam stops in a special Faraday cup mounted just downstream from the focal plane. This geometry allows us to detect protons with about 8 – 20 MeV of energy loss, which includes the region of greatest interest.

Several techniques were used to reduce background, which was the greatest challenge of this experiment. A very good low-halo beam tune was achieved, and shielding was used between the Faraday cup and wire chambers. Most important, we used an active collimator developed at IUCF. Protons scattering from this collimator, which amounted to more than 75% of the detected events, could be tagged and discriminated against. Good energy resolution is also an important requirement. We achieved an on-line resolution of 35 keV, with improvements possible when careful off-line calibrations are performed.

The primary target was a  $4.0 \pm 0.7$  mg/cm<sup>2</sup> self-supporting foil of highly enriched (97.69%)  $^{48}\text{Ca}$ . Over 20 hours of data were collected with this target in transmission mode. An on-line spectrum including  $0^\circ - 2^\circ$  data appears in Fig. 3. As expected, the

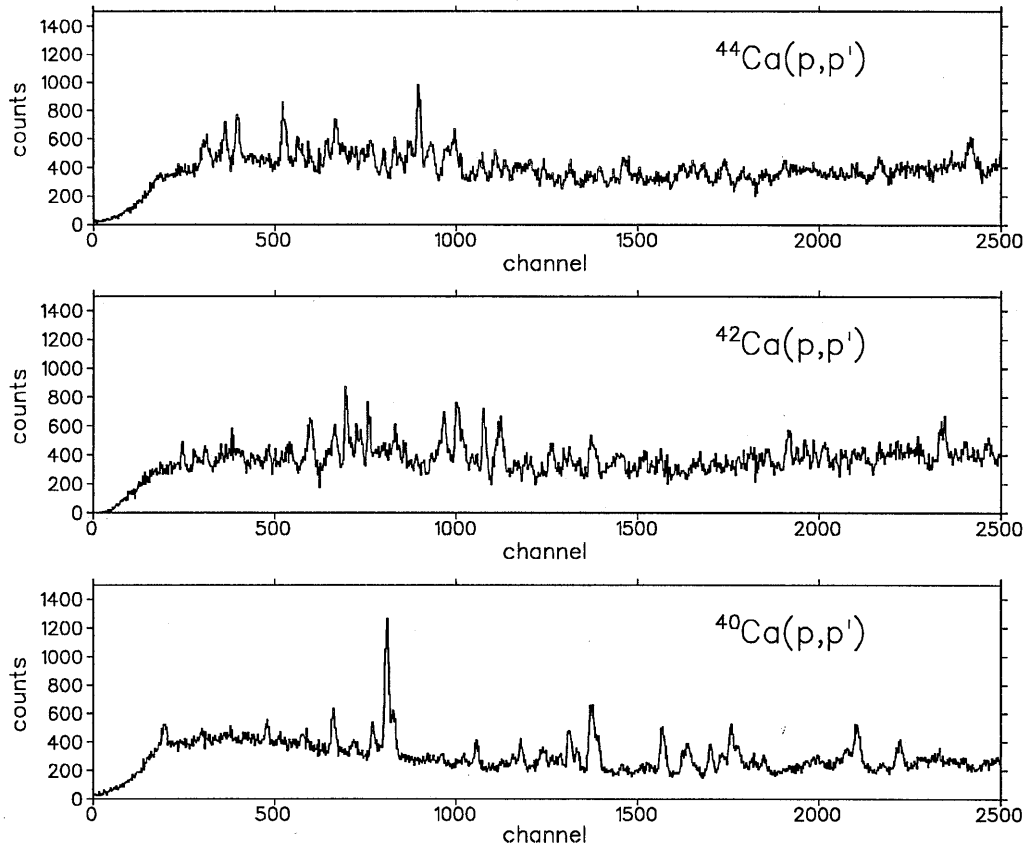


Figure 4. On-line spectra from (p,p') on  $^{44}\text{Ca}$ ,  $^{42}\text{Ca}$ , and  $^{40}\text{Ca}$  targets at very forward angles. In all three cases the M1 strength is highly fragmented. Some small periodic structures are artifacts of the on-line reconstruction algorithm.

10.21 MeV peak is the most prominent feature at this very forward angle. The experimental background is significantly improved from that shown in Fig. 1. Several much smaller peaks are visible near the main peak (see detail). The largest of these has an area 3.8% as large as the main peak. The smallest plainly visible peaks have an area about 1% as large as the main peak. Several of these small peaks are candidates for fragmented M1 strength. Analysis, which is in progress at the University of Colorado, will include separation of data into scattering-angle bins, and comparison with the earlier data at larger angles. This should give positive identification of any concentrations of M1 strength.

Other calcium targets included  $3.2 \pm 0.3 \text{ mg/cm}^2$   $^{44}\text{Ca}$  (98.68%),  $3.5 \pm 0.5 \text{ mg/cm}^2$   $^{42}\text{Ca}$  (93.71%), and  $2.9 \pm 0.3 \text{ mg/cm}^2$   $^{40}\text{Ca}$  (99.97%). On-line spectra from these are shown in Fig. 4. In  $^{44}\text{Ca}$  a simple shell model would predict a single  $\nu(f_{5/2}, f_{7/2}^{-1})$  transition with half the strength found in  $^{48}\text{Ca}$ , but instead the strength is completely fragmented. The case is similar for  $^{42}\text{Ca}$ . In view of the degree of fragmentation in these nuclei, it would indeed be unusual if there were no fragmentation whatsoever in  $^{48}\text{Ca}$ . Peaks are even visible in  $^{40}\text{Ca}(p,p')$ , including a particularly strong peak near 10.21 MeV, although no M1 strength is necessarily expected to occur here.

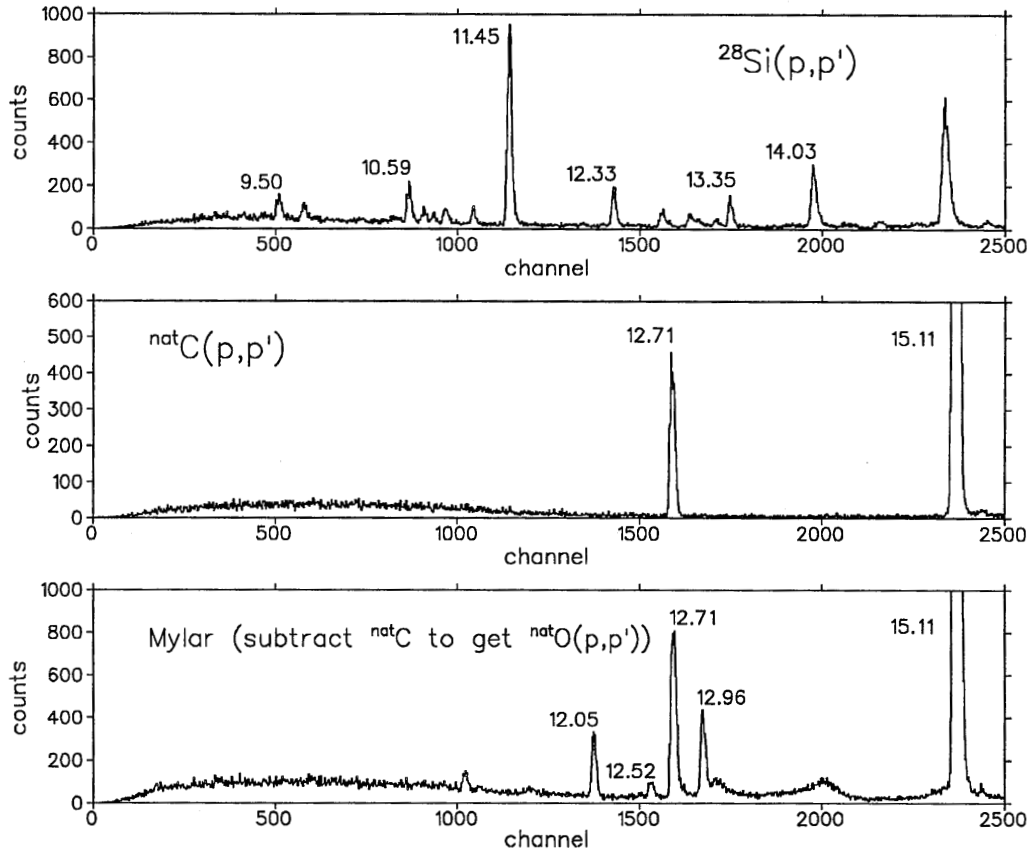


Figure 5. On-line spectra from (p,p') on  $^{28}\text{Si}$ ,  $^{\text{nat}}\text{C}$ , and Mylar targets at very forward angles. These are useful for energy calibration and removal of background and artifacts. Energy levels in  $^{28}\text{Si}$  are from Ref. 10.

To provide energy calibration and assurances against contaminant peaks we have also collected data with targets of  $5.7 \pm 0.2 \text{ mg/cm}^2$   $^{28}\text{Si}$ ,  $3.0 \pm 0.2 \text{ mg/cm}^2$   $^{\text{nat}}\text{C}$ , and Mylar. On-line spectra from these appear in Fig. 5. Silicon has many known peaks and will aid in linearizing the energy spectra. The most likely non-Ca contaminants in the Ca targets are  $^{16}\text{O}$  and  $^{12}\text{C}$ , which fortunately have no strong  $\Delta L = 0$  transitions in the region of interest. The amounts of these contaminants can be determined from large-angle ( $21^\circ$ ) data taken with the Ca and background targets. Contaminant spectra will be removed from the  $^{48}\text{Ca}$  spectra at smaller angles, although any such corrections are expected to be very small.

1. G.M. Crawley, N. Anantaraman, A. Galonsky, C. Djalali, N. Marty, M. Morlet, A. William and J.-C. Jourdain, Phys. Lett. **127B**, 322 (1983).
2. Y. Fujita, M. Fujiwara, S. Morinobu, T. Yamazaki, T. Itahashi, H. Ikegami and S.I. Hayakawa, Phys. Rev. C **37**, 45 (1988).
3. G. Eulenberg, D.I. Sober, W. Steffen, H.-D. Gräf, G. Külchler, A. Richter, E. Spamer, B.C. Metsch, and W. Knüpfer, Phys. Lett. **116B**, 113 (1982).

4. W. Steffen, H.-D. Gräf, A. Richter, A. Härting, W. Weise, U. Deutschmann, G. Lahm, and R. Neuhausen, Nucl. Phys. **A404**, 413 (1983).
5. E. Caurier, A.P. Zuker, A. Poves, and G. Martínez-Pinedo, Phys. Rev. C **50**, 225 (1994); E. Caurier, personal communication.
6. Y. Fujita, M. Fujiwara, S. Morinobu, T. Yamazaki, T. Itahashi, S. Imanishi, H. Ikegami, and S.I. Hayakawa, Phys. Rev. C **25**, 678 (1982).
7. G.P.A. Berg, W. Hürlimann, I. Katayama, S.A. Martin, J. Meissburger, J. Römer, B. Styczen, F. Osterfeld, G. Gaul, R. Santo and G. Sondermann, Phys. Rev. C **25**, 2100 (1982).
8. K.E. Rehm, P. Kienle, D.W. Miller, R.E. Segel, and J.R. Comfort, Phys. Lett. **114B**, 15 (1982).
9. D.J. Mercer, A. Galnosky, K. Ieki, G.H. Yoo, G.P.A. Berg, S. Chang, E.J. Stephenson, and J. Liu, IUCF Sci. and Tech. Rep. May 1992 - April 1993, p. 31.
10. N. Anantaraman, B.A. Brown, G.M. Crawley, A. Galonsky, C. Djalali, N. Marty, M. Morlet, A. Willis, J.-C. Jourdain, and B.H. Wildenthal, Phys. Rev. Lett. **52**, 1409 (1984).